Stretched-Exponential Photoconductivity Decay in Nanocrystalline Indium Oxide

Ekaterina FORSH[1,2,*], Alexander ILYIN[1], Mikhail MARTYSHOV[1,2], Pavel FORSH[1,2], Pavel KASHKAROV[1,2,3]

[1]*Lomonosov Moscow State University*
[2]*National Research Center "Kurchatov Institute"*
[3]*Moscow Institute of Physics and Technology*
forsh_kate@vega.phys.msu.ru

Abstract. **- The effect of ultraviolet light irradiation on the conducting properties of the nanocrystalline In_2O_3 is studied. Nanocrystalline indium oxide thin films with various nanocrystals size are prepared by sol-gel method. The mean nanocrystals size varies from 7-8 nm to 18-20 nm depending on conditions of their preparation. A large increase in conductivity by two to four orders of magnitude (depending on the nanocrystals size) is observed with light irradiation. The highly conductive state persists for a timescale of hours at room temperature after illumination. The relaxation rate of this persistent conducting state depends strongly on temperature and environment. The time-dependence of photoconductivity decay in our nanocrystalline In_2O_3 is governed by the stretched-exponential (William-Watts) relation. The stretched-exponential photodecay can be attributed to the motion of oxygen which exhibits dispersive diffusion with a characteristic power-law time dependence.**

Index Terms **— light irradiation, nanocrystalline indium oxide, oxygen diffusion, persistent photoconductivity, stretched-exponential relaxation.**

V. INTRODUCTION

The nanocrystalline indium oxide (In_2O_3) is being extensively studied for its application in sensors, light emitting diodes, liquid crystal displays and solar cells [1, 2]. However, despite these numerous applications, some fundamental properties of nanocrystalline In_2O_3 remain unclear. In particular transient photoconductivity in nanocrystalline In_2O_3 is still not fully understood. In case of nanoscale In_2O_3 photoconductive properties differ drastically from those observed in bulk materials. The contribution from the surface, acting as a trapping and recombination region for excited charge carriers, becomes dominant. It is known that persistent photoconductivity (PPC) - a light-induced change in conductance persisting after irradiation has stopped - is observed in a variety of semiconductors including wide gap metal oxides [3, 4].

One common explanation for PPC is associated with the donor complex (DX) model, and the DX centers [3], the defects whose energy depends on whether they are neutral or negatively charged. The energy of the center is lowered by removing electrons from a donor, resulting in a metastable state that is separated by a potential barrier from a neutral donor, promoting the induced conductance. In another model the origin of PPC is explained by charge separation due to traps by random potential fluctuations, which may be related to the microstructure of the films [5]. An entirely different mechanism, oxygen photoreduction, has been proposed for amorphous In_2O_3 films [6]. In this model, UV illumination in vacuum or inert gas reduces the film, creating oxygen vacancies and dramatically increases the conductivity, which restored by exposing the sample to ozone or oxygen plasma.

In the present study, we investigate the structural and photoelectrical properties of indium oxide with different nanocrystals size on purpose to clarify mechanism of photorelaxation and to find out the correlations between the microstructure parameters and electrical response to UV illumination.

VI. EXPERIMENTAL

The nanocrystalline samples of In_2O_3 were prepared by sol-gel method and then annealed at various temperatures (T=300-700 °C) during 24 h [7]. The phase composition, dispersion degree, particle size, and specific surface area of nanocomposites were studied.

The composition and the dispersion degree of the samples were determined by X-ray diffraction (XRD) using Cu K_α radiation (λ = 0.15418 nm). The XRD data were used also for estimation of In_2O_3 average grain size which was calculated from Scherrer equation. The specific surface area of the samples was estimated by the method of low-temperature nitrogen adsorption using Brunauer–Emmett–Teller model [8]. The experiments were carried out using Chemisorb 2750 (Micromeritics) unit. The morphology and nanoctystals size of the In_2O_3 samples were determined by transmission electron microscopy (TEM) using FEI Tecnai $G_2$30 TEM/STEM microscope.

In order to measure the photoelectrical characteristics, the obtained materials were deposited in the form of thin films with a thickness of ~ 1 μm over functional glass substrates. Gold contacts were vapor-deposited on the top of the films surface. Light irradiation of the nanocrystalline In_2O_3 samples were performed with UV diode with a maximum intensity at 380 nm. The conductivity measurements were performed in an air and in a vacuum of 10^{-4} Torr in a dc mode at a constant voltage of 1 V using Keithley 6487 unit. The value of the photoconductivity ($\Delta\sigma_{ph}$) was defined as the difference between the conductivity of the sample during illumination (σ_{ill}) and dark conductivity (σ_d):

$$\Delta\sigma_{ph} = \sigma_{ill} - \sigma_d . \qquad (1)$$

III. RESULTS AND DISCUSSION

The XRD patterns of the In_2O_3 samples (Fig. 1) show a single phase of cubic In_2O_3, and the peaks indicate its good crystallinity. The nanocrystals size increases while the annealing temperature rises. The calculated lattice parameter (a = 1.018 nm) for the sample is in a good agreement with the known lattice parameter for crystalline In_2O_3 (a = 1.0117 nm). The designations of the samples, annealing temperatures, nanocrystals sizes and specific surface areas are given in Table 1.

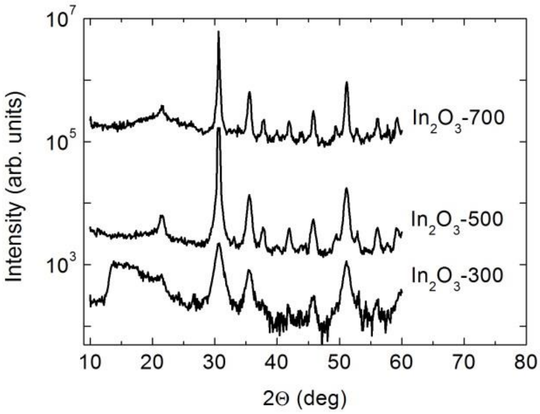

Fig. 1. X-ray diffraction patterns of In_2O_3 samples.

Table 1. The designations of samples, annealing temperatures, sizes of nanocrystals and specific surface areas.

Designation of sample	Annealing temperature (°C)	Nanocrystal size (nm)	Specific surface area (m^2/g)
In_2O_3-300	300	7-8	100
In_2O_3-500	500	12-13	35
In_2O_3-700	700	18-20	10

In order to obtain some more detailed information on the microstructure of the materials being studied, In_2O_3 samples were investigated using a transmission electron microscope (Fig. 2). The TEM analysis shows that the In_2O_3 powders consist of nanoparticles, really corresponding to cubic modification. The most probable (more than 80%) sizes of In_2O_3 nanoparticles in the In_2O_3-300 sample are within 5-10 nm which corresponds to XRD analysis (see Table 1).

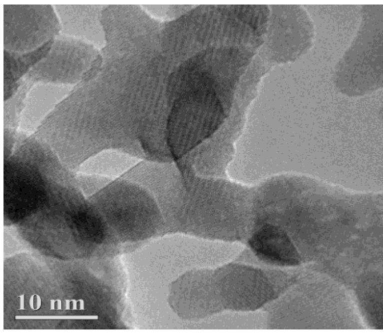

Fig. 2. TEM image of In_2O_3-300 sample.

Typical photoconductivity behavior of the investigated samples under illumination is presented in Fig. 3.

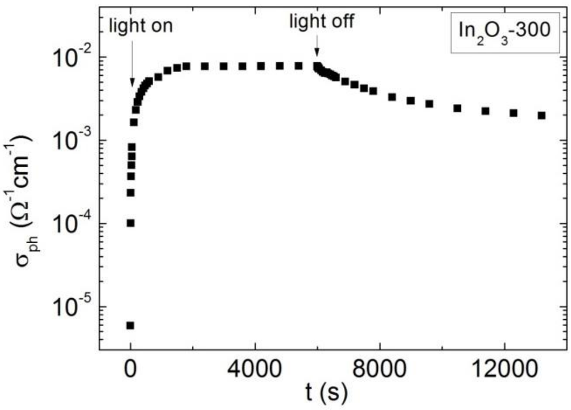

Fig. 3. Time evolution of conductivity of the nanocrystalline In_2O_3-300 sample.

An increase in conductivity occurs rather quickly to reach a value more than three orders of magnitude larger than before. When the light is turned off, it recovers slightly but remains at values higher than before light irradiation. So we can see robust PPC at room temperature. At the same time the value of the photoconductivity increases and the persistent photoconductivity decreases with the nanocrystals size reduction (see Fig. 4).

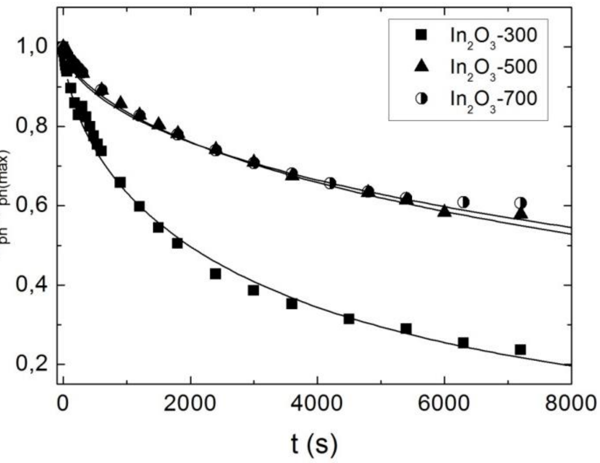

Fig. 4. The photoconductivity decay of In_2O_3 films in air. Solid lines are the best-fit lines with Eq. (2).

The presented on Fig. 4 dependencies can be approximated by exponents "stretched" in time :

$$\Delta\sigma_{ph} = \sigma_0 \exp\left[-\left(t/\tau\right)^{\beta}\right], \qquad (2)$$

where τ is the "effective" relaxation time, β a parameter that characterizes the nonhomogeneous of the system. The equation (2) is often termed William-Watts [9] or Kohlrausch [10] relaxation.

All spectra in the Fig. 4 could be well approximated by (2). The values of τ and β are given in Table 2. As we can see the values of the effective relaxation time are strongly depend on the nanocrystals size, at the same time the values of β do not practically depend on the nanocrystals size.

Table 2. The values of the effective relaxation time and the exponent parameter for In_2O_3 samples.

Sample	τ, s	β
In_2O_3-300	$3{,}6\cdot10^3$	0,63
In_2O_3-500	$1{,}9\cdot10^4$	0,57
In_2O_3-700	$2{,}1\cdot10^4$	0,55

The effective relaxation time τ follows Arrhenius behavior with the activation energy of about 0.23 eV for all In_2O_3 samples (Fig. 5).

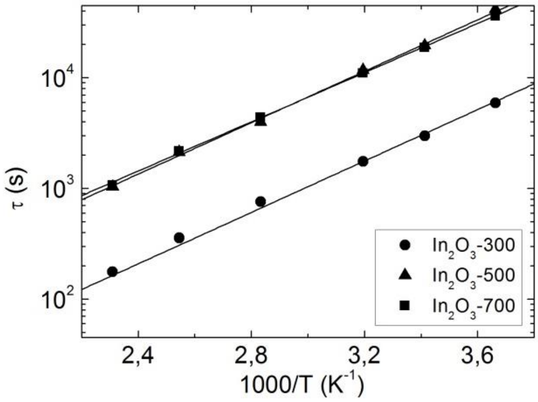

Fig. 5. The temperature dependences of the effective relaxation time for the nanocrystalline In_2O_3. Solid lines are the best-fit lines with Arrhenius plot.

The temperature dependences of dc conductivity of the In_2O_3-300 with nanocrystals different in size before and after light illumination are presented in Fig. 6 (for the other samples the similar dependences have been obtained).

For the thermally activated band conduction, the conductivity (σ_{dc}) can be expressed as:

$$\sigma_{dc} = \sigma_0 \exp\left(-E_A / k_B T\right) \qquad (3)$$

where E_A denotes the thermal activation energy of electrical conduction, σ_0 represents a parameter depending on the semiconductor nature and k_B is the Boltzmann constant.

As we can see, before light illumination the conductivity of the In_2O_3 sample is lower and the activation energy is higher than those after light irradiation. The values of the activation energies for all samples are given in Table 1. In case of electrons transfer over the conduction band the thermal activation energy of electrical conductivity is defined as the energy difference between the bottom of the conduction band E_C and Fermi

level E_F approximated to absolute zero temperature [11]:

$$E_A = \left(E_C - E_F\right)_0 . \qquad (4)$$

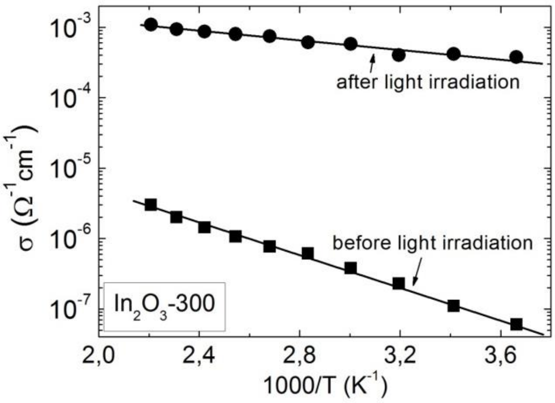

Fig. 6. The temperature dependences of conductivity of the In_2O_3-300 sample. Solid lines are the best-fit lines with Eq. (3)

Consequently, the increase of the activation energy E_A during the light illumination can be explained by Fermi level shift closer to the bottom of the conduction band as a result of the increase of the free electron concentration.

In order to obtain some more detailed information on the influence of the atmosphere to photorelaxation in nanocrystalline indium oxide the kinetics of the decay of the photoconductivity were measured in air and in vacuum at room temperature (Fig. 7). It is evident that conductivity decay in vacuum is much slower and persistent photoconductivity is much higher than those in air. It may indicate that the adsorbed oxygen species play a key role in the observed phenomena.

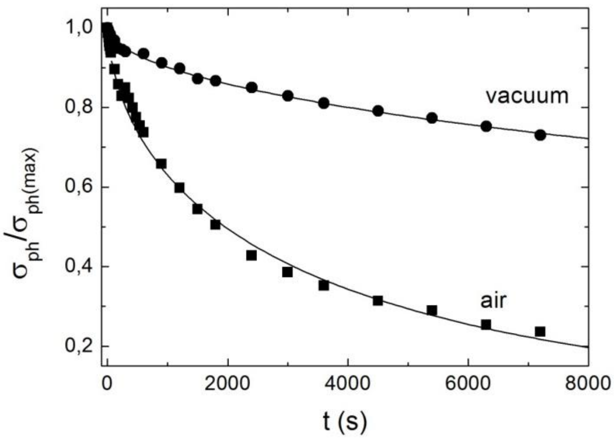

Fig. 7. The photoconductivity decay in air and in vacuum for the In_2O_3-300 sample. Solid lines are the best-fit lines with Eq. (2).

Now we discuss the origin of the observed photoinduced conductivity and stretched-exponential photorelaxation in the In_2O_3 films. As is always the case for *n*-type semiconductors, oxygen adsorbs on the surface and traps some of the carriers to become a negative ion on the surface or at the grain boundary. During UV light irradiation holes and electrons generate inside the grain.

These hole carriers migrate to the grain boundary and react with the adsorbed oxygen, so that oxygen can desorb according to the reaction $h^+ + O_2^- \rightarrow O_2 \uparrow$, where h^+ is the photogenerated hole carrier. Besides, there are nonequilibrium electrons inside the grain after turning off the light, so that increases the free electrons concentration and consequently the conductivity of the In_2O_3 films. Since desorbed oxygen can't return on grain boundary in vacuum after turning off the light, the high-conducting state remains.

We propose that the stretched-exponential relaxation we observe may be related to correlated oxygen motion inside the film placed in the air atmosphere. For small departures of electron concentration from equilibrium, the decay should be given by the linear relation

$$\frac{d\Delta n}{dt} = -\nu(t)\Delta n, \quad (5)$$

where $\nu(t)$ is equilibration rate.

The stretched-exponential relaxation commonly observed in disordered systems is explained by time-dependent atomic diffusion. In particular, relaxation in amorphous hydrogenated silicon is attributed to the motion of bonded hydrogen which exhibit dispersive diffusion characterized by a power-law time decay [12-15]. In our case we argue that the oxygen demonstrates a power-law dispersive diffusion. Namely oxygen diffuses inside the film, moving by hopping between a localized states.

According to this model the rate constant $\nu(t)$ will be proportional to the oxygen hopping rate D/a^2, where *a* is a characteristic hopping distance that the oxygen moves in a single diffusion step and *D* is the diffusion coefficient.

The results [13] show that

$$D = D_0(\omega_0 t)^{-\alpha}, \quad (6)$$

where ω_0 is an attempt frequency, α is dispersive parameter.

From the oxygen diffusion data we set the equilibrium rate as

$$\nu(t) = \frac{D_0}{a^2}\left(\omega_0 t\right)^{-\alpha}. \quad (7)$$

Inserting Eq. (5) and Eq. (7) and integrating immediately yields

$$\Delta n = n_0 \exp\left[-\left(t/\tau\right)^{\beta}\right], \quad (8)$$

where $\beta = 1-\alpha$.

According to [16]

$$\sigma_{ph} = en\mu,$$

where μ is electron mobility, we get

$$\Delta\sigma_{ph} = \sigma_0 \exp\left[-\left(t/\tau\right)^{\beta}\right].$$

Thus the stretched-exponential decay follows directly from the dispersive diffusion mechanism.

Following the analogy to the dispersive transport of charge carriers, we argue that the dispersive diffusion of oxygen arises from a broad distribution of release times. Differences in the local atomic configurations should yield a distribution of activation energies for the motion of oxygen. When the distribution is broad, the oxygen motion will become slower at longer times. Furthermore, if the dispersion in *D* arises from an exponential distribution of site energies $\exp\left(-E/k_B T_0\right)$, where $k_B T_0$ is the width of the trap distribution, then the theory [15] predicts that

$$1-\alpha = \beta = T/T_0$$

Figure 8 shows the temperature dependence of the exponent β for the nanocrystalline In_2O_3-500 (for the other samples the similar dependences have been obtained). The solid line in β vs *T* shown in Fig. 8 is consistent with $T_0 \approx 514$ K.

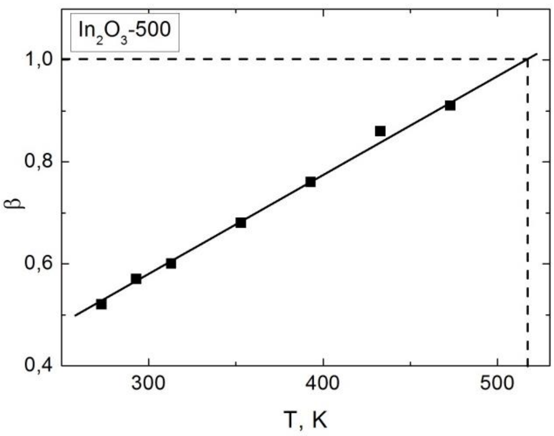

Fig. 8. The temperature dependence of the exponent β for the In_2O_3-500 sample.

To summarize the model, we describe the diffusion of oxygen in terms of a distribution of bond energies, and then relate the time dependence of *D* to the electronic relaxation. In this way the stretched exponential derives from a physically plausible exponential distribution of bond energies, and a direct connection between the structure and the electronic relaxation is found.

IV. CONCLUSION

In conclusion, we observed a large enhancement in the conductivity by UV irradiation of the nanocrystalline indium oxide thin films with various nanocrystals size. After light was turned off we observed robust photoconductivity in the nanostructured In_2O_3 which persists for many hours at room temperature. The value of the photoconductivity increased and the persistent photoconductivity decreased with the nanocrystals size reduction. We showed that the slow photorelaxation in the nanocrystalline In_2O_3 was accurately characterized by a stretched-exponential function that could be explained by the correlated oxygen motion inside the film.

REFERENCES

[1] H.L. Hartnagel, A.L. Dawar, A.K. Jain, and C. Jagadish, *Semiconducting Transparent Thin Films*, Institute of Physics, Bristol, 1995.

[2] M.N. Martyshov, E.A. Forsh, A.V. Marikutsa, P.A. Forsh, M.N. Rumyantseva, A.M. Gaskov, and P.K. Kashkarov "Influence of In_2O_3 Nanocrystals Size on the Sensitivity to NO_2", *J. of Nanoelectronics and Optoelectronics*, vol. 6, p. 452, 2011.

[3] D.V. Lang and R.A. Logan, "Large-Lattice-Relaxation Model for Persistent Photoconductivity in Compound Semiconductors", *Phys. Rev. Lett*, vol. 39, p. 635, 1977.

[4] J.M. Bian, X.M. Li, X.D. Gao, W.D. Yu, and L.D. Chen, "Deposition and Electrical Properties of N–In codoped *p*-type ZnO Films by Ultrasonic Spray Pyrolysis", *Appl. Phys.Lett.*, vol. 84, p. 541, 2004.

[5] C. Kisielowski, J. Kruger, S. Ruvimov, T. Suski, J.W. Ager, E. Jones, Z. Liliental-Weber, M. Rubin, E.R. Weber, M.D. Bremser, and R.F. Davis "Strain-Related Phenomena in GaN Thin Films", *Phys. Rev. D*, vol. 54, p. 17745, 1996.

[6] B. Pashmakov, B. Claflin, H. Fritzsche, "Photoreduction and Oxidation of Amorphous Indium Oxide", *Solid State Commun.*, vol. 86, p. 619, 1993.

[7] E. A. Forsh, A. V. Marikutsa, M. N. Martyshov, P. A. Forsh, M. N. Rumyantseva, A. M. Gas'kov, and P. K. Kashkarov, "Charge Carrier Transport in Indium Oxide Nanocrystals", *JETP*, vol. 111, No. 4, p. 653. (2010)

[8] S. Brunauer, *The Adsorption of Gases and Vapors*, Princeton University Press, Princeton, 1943.

[9] G. Williams and D.C. Watts, "Non-symmetrical Dielectric Relaxation Behaviour Arising from a Simple Empirical Decay Function", *Trans. Faraday Soc.*, vol. 66, p. 80, 1970

[10] R. Kohlrausch, "I. Ueber das Dellmann'sche Elektrometer", *Ann. Phys. (Leipzig)*, vol. 72, p. 353 (1847).

[11] M.H. Brodsky, *Amorphous Semiconductors*, Springer-Verlag, Berlin, Heidelberg, New York, 1979.

[12] J. Kakalios, R.A. Street, and W.B. Jackson, "Stretched-Exponential Relaxation Arising from Dispersive Diffusion of Hydrogen in Amorphous Silicon", *Phys. Rev. Lett.*, vol. 59, p. 1037, 1987.

[13] H. Scher and E. W. Montroll, "Anomalous Transit-Time Dispersion in Amorphous Solids", *Phys. Rev. B*, vol. 12, p. 2455, 1975.

[14] Michael F. Shlesinger, Elliott W. Montroll, "On the Williams—Watts function of dielectric relaxation", *Proc Natl Acad Sci U S A.*, vol. 81(4), p. 1280, 1984.

[15] Joseph Klafter, Michael F. Shlesinger, "On the relationship among three theories of relaxation in disordered systems", *Proc Natl Acad Sci U S A.*, vol. 83(4), p. 848, 1986.

[16] V.L. Bonch-Bruevich, S.G. Kalashnikov, *The Physics of Semiconductors*, Nauka, Moscow, 1990.